

Article

Durability of Pultruded GFRP through Ten-Year Outdoor Exposure Test

Itaru Nishizaki, Hiroki Sakuraba * and Tomonori Tomiyama

Received: 1 July 2015; Accepted: 20 November 2015; Published: 30 November 2015
Academic Editors: Raafat El-Hacha and Alexander Böker

Public Works Research Institute, 1-6 Minamihara, Tsukuba, Ibaraki 305-8516, Japan; nisizaki@pwri.go.jp (I.N.); tomiyama@pwri.go.jp (T.T.)

* Correspondence: hiro-sakura@pwri.go.jp; Tel.: +81-29-879-6763 (ext. 4129); Fax: +81-29-879-6733

Abstract: Pultrusion is an easy molding method of fiber-reinforced polymer (FRP) to obtain a long composite material with a uniform cross-section at relatively low cost. In some cases, pultruded FRPs are now used in bridges and deck projects. Since the application of pultruded FRP as a structural material is increasing, a study on the durability of pultruded FRP under outdoor conditions is necessary in terms of safety. Some studies have shown that pultruded glass fiber-reinforced polymer (GFRP) exhibits a slight reduction in mechanical properties during outdoor exposure. Since pultruded GFRP consists of multi-layers, the change of mechanical properties in each layer is important to understand. In this study, an outdoor exposure test on pultruded GFRP for 10 years was conducted with three types of pultruded GFRP, which have different laminate systems, including surface-coated specimens of each type. Changes of strength and elastic modulus due to outdoor exposure were discussed with a focus on the contribution of each layer based on the rule of mixtures.

Keywords: pultrusion; GFRP; ten-year outdoor exposure; laminate system; mechanical properties

1. Introduction

Recently, the use of fiber-reinforced polymer (FRP) as a structural material has increased due to its high resistance to corrosion and low weight. Pultrusion of FRP is a particularly easy method that can produce long sections of material with a uniform cross-section at relatively low cost. This makes FRP a structural material which can be used for construction. Information on the durability of pultruded FRP is important for using FRP safely. There were some studies on the durability of pultruded FRP used for construction with mainly glass fibers [1–5], but many of them only focused on moist environments. When the durability of FRP in an ambient condition is considered, an outdoor exposure test is an important way to understand the durability. As for the use of glass fiber-reinforced polymer (GFRP) reinforcement, GFRP bars embedded in concrete for seven years were investigated to assess the structural reliability of a bridge deck reinforced with GFRP bars [6,7]. Some studies on the durability of press-molded or hand lay-up GFRP investigated by outdoor exposure tests were also reported [8–10].

A six-year outdoor exposure test for pultruded GFRP was conducted by the authors [11], and it was shown that a surface coating has a protective effect and reduces the deterioration of mechanical properties and that uncoated GFRP showed a slight reduction of mechanical properties. However, in the six-year outdoor test, deteriorated layers of pultruded GFRP were not investigated although they consisted of multi-layers.

This study presents an outdoor exposure test on pultruded GFRP for 10 years to investigate layers of GFRP which can deteriorate during outdoor exposure. Three types of pultruded GFRP, with different laminate systems, were tested, including painted specimens of the GFRP. By calculating the

contribution ratios of each layer based on the rule of mixtures, deteriorations of strength and elastic modulus of the pultruded GFRP are discussed.

2. Experimental Section

2.1. Specimen

Pultruded GFRP plates made of E-glass fibers and vinyl ester resin, which is bisphenol A with styrene solvent, were used to prepare the specimens in this study. Each plate was 420 mm wide, 3.2 mm thick. The laminate systems consist of the combination of three fiber types: continuous strand mat with random fiber directions, plain-woven cloth with bidirectional fibers and unidirectional roving, as shown in Figure 1. Table 1 shows three laminate systems that were used in this study. Note that since the percentages of “Layer system and fiber type” are approximate values, the percentages in R26 do not add up to exactly 100%. These plates were cut into 620-mm-length specimens. In this study, the direction corresponding to the direction of pultrusion is defined as the 0° direction, and the lateral direction of pultrusion is therefore defined as the 90° direction.

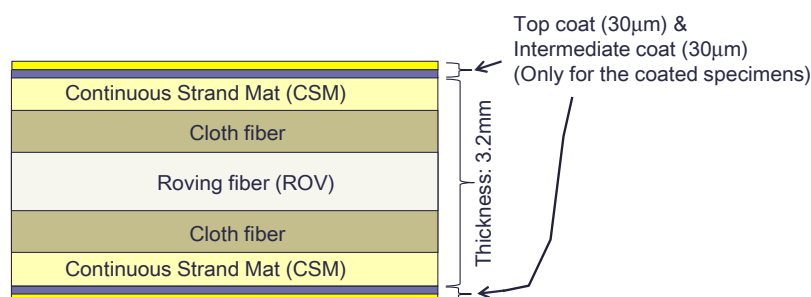


Figure 1. A schematic illustration of cross-section of the specimens.

Table 1. Laminate system of the specimens.

Code	V_f (%)	Layer System and Fiber Type (the Values Show the Volume Fiber Content Ratio of the Corresponding Layer in Volume Fraction)
R43	43	CSM 9.5%/Cloth 19%/ROV 43%/Cloth 19%/CSM 9.5%
R26	39	CSM 16%/Cloth 21.5%/ROV 26%/Cloth 21.5%/CSM 16%
R12	36	CSM 21%/Cloth 23%/ROV 12%/Cloth 23%/CSM 21%

Coated and uncoated specimens were also prepared for all cases. Coated specimens were coated with an epoxy intermediate coating with a designed thickness of 30 μm and then coated with an acrylurethane resin top coating with a designed thickness of 30 μm by using a brush. The thicknesses of the intermediate and the top coating were determined based on manufacturer’s specification and controlled by measuring their weights. The actual thicknesses of the intermediate and the top coating were measured by using a digital stereomicroscope, and it was confirmed that the actual thicknesses had a range from 70 to 75 μm. Two sets of specimens were prepared for all cases.

An exposure test was carried out for 10 years (from June 2003 to July 2013), in Tsukuba, which is located near Tokyo and has a moderate climate with an annual mean temperature of 14.3 °C and an annual rain fall of 1326 mm. The exposure test was first started to investigate the safety of pultruded GFRP for use as a structural material. Figure 2 shows the maximum, average and minimum temperatures at the Tsukuba exposure site. The temperatures were measured at intervals of one hour for 10 years, and they were averaged monthly. The maximum and minimum temperatures reached 31.5 and −3.1 °C, respectively, as shown in Figure 2.

The specimens were placed facing south on a 5° slope using steel exposure racks, and Figure 3 shows specimens placed by using the steel exposure racks. One set of specimens was retrieved after one year and the other set was retrieved after 10 years.

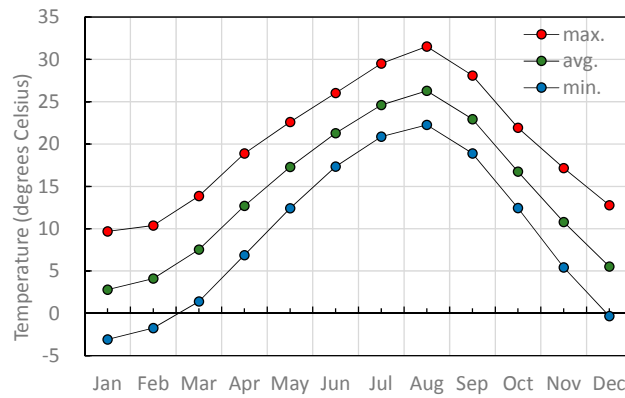


Figure 2. Maximum, average and minimum temperatures each month at Tsukuba exposure site.



Figure 3. Specimens placed on exposure racks facing south on a 5° slope.

Table 2 shows the tensile strength and modulus of the raw materials that are provided by the manufacturers and used to design the laminate systems. Despite the same fiber, the tensile modulus and strength of the continuous strand mat (CSM) are lower than those of the glass fiber because the CSM has random fiber directions.

Table 2. Mechanical properties of each layer of the specimens.

Mechanical Properties	Glass Fiber	Continuous Strand Mat (CSM)	Matrix Resin
Tensile modulus (GPa)	75	26.9	1.875
Tensile strength (MPa)	2,500	188.5	62.5

Tensile modulus and strength based on the rule of mixtures were calculated by Equations (1) and (2). The rule of mixtures is usually used for unidirectional FRP, but in this study it was used to calculate the contribution ratios of each layer in the laminates. The contribution of plain-woven cloth was divided by two because half of the fibers are oriented to the lateral direction of the testing direction. Upon calculating the tensile modulus and strength for the 90° direction, V_{TOV} was assumed to be zero because the roving layer can contribute mainly to the 0° direction. In Equation (2), the empirical coefficient for tensile strength is usually obtained by a test and the previous studies [12] suggest that the coefficient for unidirectional GFRP is approximately 0.75. Each term in Equation (2) shows the contribution of each layer to the strength, hence the ratio of contribution of each layer was calculated by Equations (3)–(6).

$$E_t = \left\{ E_f \cdot V_{rov} + \frac{E_f \cdot V_{cloth}}{2} + E_{CSM} \cdot V_{CSM} + E_m \cdot (1 - V_{rov} - V_{cloth} - V_{CSM}) \right\} \quad (1)$$

where E_t is the tensile modulus of the FRP (GPa), E_f is the tensile modulus of the glass fiber (GPa), E_m is the tensile modulus of the matrix resin (GPa), E_{CSM} is the tensile modulus of the CSM (GPa), V_{rov} is the volume fiber content ratio of the roving layer (for the tensing direction), V_{cloth} is the volume fiber content ratio of the cloth, V_{CSM} is the volume fiber content ratio of the CSM.

$$F = K \cdot \left\{ F_f \cdot V_{rov} + \frac{F_f \cdot V_{cloth}}{2} + F_{CSM} \cdot V_{CSM} + F_m \cdot (1 - V_{rov} - V_{cloth} - V_{CSM}) \right\} \quad (2)$$

where F is the tensile strength of the FRP (MPa), K is the empirical coefficient for tensile strength, F_f is the tensile strength of the glass fiber (MPa), F_m is the tensile strength of the matrix resin (MPa), F_{CSM} is the tensile strength of the CSM (MPa), V_{rov} is the volume fiber content ratio of the roving layer (for the tensing direction), V_{cloth} is the volume fiber content ratio of the cloth, V_{CSM} is the volume fiber content ratio of the CSM.

$$R_{rov} = K \cdot F_f \cdot V_{rov} / F \quad (3)$$

$$R_{cloth} = \frac{K \cdot F_f \cdot V_{cloth}}{2} / F \quad (4)$$

$$R_{CSM} = K \cdot F_{CSM} \cdot V_{CSM} / F \quad (5)$$

$$R_m = K \cdot F_m \cdot (1 - V_{rov} - V_{cloth} - V_{CSM}) / F \quad (6)$$

where R_{rov} is the contribution ratio of the roving layer, R_{cloth} is the contribution ratio of the cloth layer, R_{CSM} is the contribution ratio of the CSM layer, R_m is the contribution ratio of the matrix resin.

2.2. Testing Method

Tensile tests in the 0° and 90° directions and an in-plane shear test (tensile test at a 45° direction) were carried out, and Figure 4 shows the definition of the testing directions. The specimens retrieved from the exposure test were washed with water, and five coupons were taken for each test. Note that the portions of each plate which were within a 5 cm distance from the edges were not used for the tests to avoid disturbance from the edges.

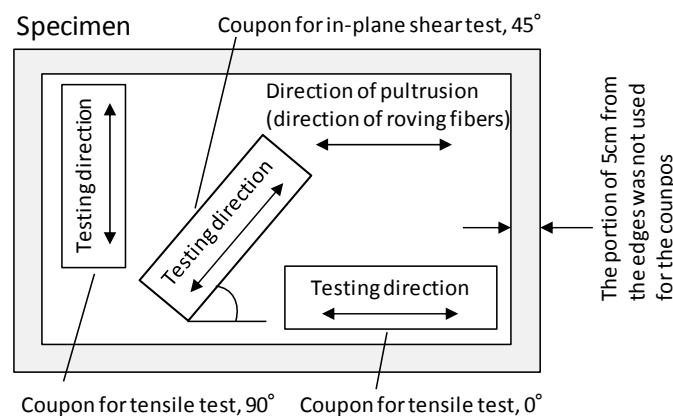


Figure 4. Test coupons cut out from the exposed specimens.

The tensile tests were carried out based on ISO 3268. The coupons were 250 mm long and 25 mm wide, and the test speed was 1 mm/min. Equation (7) was used to calculate the tensile strength. For the coated specimens, the designed thickness of the paint layer (120 μm) was subtracted from the measured value.

$$\sigma_t = \frac{P_t}{bh} \quad (7)$$

where, σ_t is the tensile strength (MPa), P_t is the maximum tensile load (N), b is the width of the coupon (mm), h is the thickness of the coupon (mm).

Equations (8) and (9) were used to calculate the coefficient of variation (CV) based on the results of five coupons.

$$CV_{ts} = \frac{SD_{ts}}{\bar{\sigma}_t} \quad (8)$$

$$CV_{tm} = \frac{SD_{tm}}{\bar{E}_t} \quad (9)$$

where CV_{ts} is the coefficient of variation for the tensile strength, SD_{ts} is the standard deviation for the tensile strength (MPa), $\bar{\sigma}_t$ is the averaged tensile strength (MPa), CV_{tm} is the coefficient of variation for the tensile modulus, SD_{tm} is the standard deviation for the tensile modulus (GPa), \bar{E}_t is the averaged tensile modulus (GPa).

The in-plane shear test (tensile test at a 45° direction) was carried out based on JIS 7059. The coupons were 250 mm long and 25 mm wide, and the test speed was 1 mm/min. Equation (10) was used to calculate the in-plane shear strength. For the coated specimens, the designed thickness of the paint layer (120 μm) was subtracted from the measured value.

$$\tau_s = \frac{P_s}{2bh} \quad (10)$$

where τ_s is the in-plane shear strength (MPa), P_s is the maximum load (N), b is the width of the coupon (mm), h is the thickness of the coupon (mm).

Equations (11) and (12) were used to calculate the coefficient of variation (CV) based on the results of five coupons.

$$CV_{ss} = \frac{SD_{ss}}{\bar{\tau}_s} \quad (11)$$

$$CV_{sm} = \frac{SD_{sm}}{\bar{G}_s} \quad (12)$$

where CV_{ss} is the coefficient of variation for the in-plane shear stress, SD_{ss} is the standard deviation for the in-plan shear stress (MPa), $\bar{\tau}_s$ is the averaged in-plane shear strength (MPa), CV_{sm} is the coefficient of variation for the in-plane shear modulus, SD_{sm} is the standard deviation for the in-plane modulus (GPa), \bar{G}_s is the averaged in-plane shear modulus (GPa).

Retention ratios are used to discuss the change of the strength and elastic modulus with aging, and they are defined in Equations (13) and (14).

$$Rr_s = \frac{f_t^{\text{exposed}}}{f_t^{0\text{year}}} \quad (13)$$

$$Rr_m = \frac{E_t^{\text{exposed}}}{E_t^{0\text{year}}} \quad (14)$$

where Rr_s is the retention ratio for the strength, f_t^{exposed} is the tensile strength or the in-plane shear strength after the exposure (MPa), $f_t^{0\text{year}}$ is the tensile strength or in-plane shear strength before the exposure (MPa), E_t^{exposed} is the tensile modulus or in-plane shear modulus after the exposure (GPa), Rr_m is the retention ratio for the elastic modulus, $E_t^{0\text{year}}$ is the tensile modulus or in-plane shear modulus before the exposure (GPa).

3. Results and Discussions

3.1. Unpainted Specimens

Test results of unpainted specimens are discussed with the contribution ratios based on the rule of mixtures. Table 3 shows the tensile strength of unpainted specimens in comparison with the calculated values. The experimental coefficient, K , was set as 1.0 for the calculation. The ratio of the experimental values over the corresponding calculated values are from 0.532 to 0.832, as shown in Table 3. The average value of the experiment/calculation ratio among the values of the 0° and 90° directions was 0.636, which was smaller than the suggested value, 0.75, for unidirectional FRP in the previous study [12].

Table 3. Tensile strength of unpainted specimens in comparison with calculated values.

Testing Direction	Code	0 Years (MPa); Coefficient of Variation, CV	Calculated Value ($K = 1$), (MPa)	Experiment/Calculation
0°	R43	409.6; CV_{ts} : 21.0%	717.5	0.571
	R26	369.0; CV_{ts} : 3.6%	524.8	0.703
	R12	319.2; CV_{ts} : 4.6%	383.5	0.832
90°	R43	135.8; CV_{ts} : 2.6%	255.3	0.532
	R26	165.8; CV_{ts} : 4.3%	271.3	0.611
	R12	156.2; CV_{ts} : 3.4%	275.5	0.567

Note that five coupons were used for each test.

Table 4 shows the tensile and in-plane shear strengths of unpainted specimens with the retention ratios. CV_{ts} and CV_{ss} of 0 years have a range from 2.6% to 4.3%, except for that of R43 of the 0° direction, which is 21.0%. In the case of one year, Rr_s shows a range from 0.91 to 1.16, and CV_{ts} and CV_{ss} range from 1.0% to 6.2%. In the case of 10 years, Rr_s shows a range from 0.67 to 1.07, and CV_{ts} and CV_{ss} range from 2.1% to 7.8%. Rr_s of R43 at the 0° direction is higher than those of the other cases probably because of its bigger CV_{ts} . Overall, Rr_s of the 90° and 45° (in-plane shear) directions show lower values than that of the 0° direction.

Table 4. Tensile and in-plane shear strengths of unpainted specimens with retention ratios.

Testing Direction	Code	Strength (MPa); Coefficient of Variation, CV			Retention Ratio, Rr_s	
		0 Years	1 Year	10 Years	1 Year	10 Years
0°	R43	409.6; CV_{ts} : 21.0%	473.7; CV_{ts} : 3.9%	440.1; CV_{ts} : 3.6%	1.16	1.07
	R26	369.0; CV_{ts} : 3.6%	370.7; CV_{ts} : 4.3%	307.1; CV_{ts} : 4.0%	1.00	0.83
	R12	319.2; CV_{ts} : 4.6%	309.2; CV_{ts} : 6.2%	266.3; CV_{ts} : 7.8%	0.97	0.83
90°	R43	135.8; CV_{ts} : 2.6%	134.1; CV_{ts} : 1.0%	104.2; CV_{ts} : 3.9%	0.99	0.77
	R26	165.8; CV_{ts} : 4.3%	150.6; CV_{ts} : 5.0%	115.4; CV_{ts} : 4.1%	0.91	0.70
	R12	156.2; CV_{ts} : 3.4%	152.6; CV_{ts} : 2.7%	119.8; CV_{ts} : 2.6%	0.98	0.77
45° (In-plane shear)	R43	52.6; CV_{ss} : 3.4%	53.1; CV_{ss} : 2.4%	40.4; CV_{ss} : 5.0%	1.01	0.77
	R26	56.9; CV_{ss} : 0.8%	62.1; CV_{ss} : 3.1%	41.7; CV_{ss} : 2.3%	1.09	0.73
	R12	58.0; CV_{ss} : 4.5%	58.0; CV_{ss} : 3.0%	38.9; CV_{ss} : 2.1%	1.00	0.67

Note that five coupons were used for each test.

Table 5 shows the contribution ratios of each layer based on the rule of mixtures calculated by Equations (3)–(6). In the case of the 0° direction, R_{rov} and R_{cloth} show dominant values, and their summations give a range from 82.2% to 93.1%. On the other hand, in the case of the 90° direction, R_{cloth} gives a range from 75.1% to 80.0%. It is thought that the reduction of Rr_s of the 90° direction in 10 years can be caused by the deterioration of plain-woven cloth because the contribution ratios of the plain-woven cloth of the 90° direction are dominant. By considering R_{cloth} of the 90° direction, Rr_s of the 45° direction (in-plane shear) in 10 years may be also reduced by the deterioration of plain-woven cloth.

Table 5. Contribution ratios of each layer based on the rule of mixtures.

Testing Direction	Code	Contribution Ratio of Each Layer (%)			
		$R_{CSM, CSM}$	R_{cloth} Plain Woven Cloth	$R_{rov, Roving}$	$R_m, Matrix$
0°	R43	2.1	28.5	64.4	5.0
	R26	4.5	39.9	48.3	7.3
	R12	7.4	54.0	28.2	10.4
90°	R43	6.0	80.0	0.0	14.0
	R26	8.7	77.3	0.0	14.1
	R12	10.3	75.1	0.0	14.5

Table 6 shows the elastic modulus of unpainted specimens with the retention ratios. CV_{tm} and CV_{sm} in 0 years have a range from 1.7% to 4.3%, except for that of R43 of the 0° direction, which is 12.3%. Rr_m of one year shows a range from 1.06 to 1.20, and a CV_{tm} range from 1.1% to 4.6%. In the case of 10 years, Rr_m shows a range from 1.01 to 1.29, and a CV_{tm} range from 2.1% to 5.8%. Rr_m is higher than those of the tensile and in-plane shear strengths, probably due to the effect of post-curing of the resin.

Table 6. Elastic modulus of unpainted specimens with retention ratios.

Testing Direction	Code	Elastic Modulus (GPa); Coefficient of Variation, CV			Retention Ratio, Rr_m	
		0 Years	1 Year	10 Years	1 Year	10 Years
0°	R43	20.9; CV_{tm} : 12.3%	25.0; CV_{tm} : 3.2%	26.9; CV_{tm} : 5.2%	1.20	1.29
	R26	19.2; CV_{tm} : 4.3%	20.5; CV_{tm} : 2.0%	20.2; CV_{tm} : 2.5%	1.07	1.05
	R12	17.9; CV_{tm} : 2.5%	19.0; CV_{tm} : 3.5%	18.7; CV_{tm} : 5.8%	1.06	1.04
90°	R43	12.5; CV_{tm} : 2.5%	13.4; CV_{tm} : 1.4%	13.4; CV_{tm} : 1.4%	1.07	1.07
	R26	12.9; CV_{tm} : 4.0%	13.6; CV_{tm} : 1.1%	13.9; CV_{tm} : 2.1%	1.06	1.07
	R12	12.8; CV_{tm} : 2.3%	14.3; CV_{tm} : 1.1%	13.4; CV_{tm} : 2.1%	1.12	1.05
45° (In-plane shear modulus)	R43	3.40; CV_{sm} : 3.4%	4.05; CV_{sm} : 2.8%	4.01; CV_{sm} : 2.9%	1.19	1.18
	R26	3.76; CV_{sm} : 1.7%	4.17; CV_{sm} : 1.6%	3.80; CV_{sm} : 1.4%	1.11	1.01
	R12	3.49; CV_{sm} : 2.9%	4.10; CV_{sm} : 4.6%	3.80; CV_{sm} : 2.7%	1.17	1.09

Note that five coupons were used for each test.

Figure 5 summarizes results of unpainted specimens. It is shown that, overall, the strength of the unpainted specimens declines after 10 years of outdoor exposure as shown in Table 4, and that the plain-woven cloth layers were deteriorated during 10 years of outdoor exposure by considering the contribution ratios of each layer calculated based on the rule of mixtures. On the other hand, the elastic modulus of the unpainted specimens shows a slight increase as shown in Table 6.

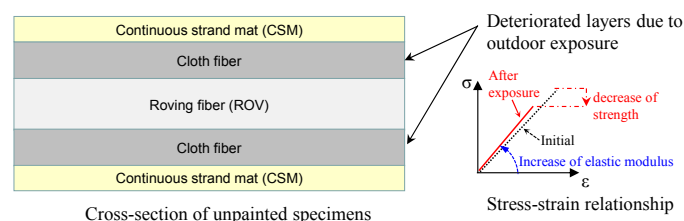


Figure 5. Summary of results of unpainted specimens.

3.2. Painted Specimens

Test results of painted specimens are discussed by comparing them with the results of the unpainted specimens. Table 7 shows the tensile and in-plane shear strengths of painted specimens with retention ratios. In the case of one year, Rr_s shows a range from 0.92 to 1.21, and CV_{ts} and CV_{ss} range from 2.0% to 10.7%. In the case of 10 years, Rr_s shows a range from 0.86 to 1.24, which are higher values than those of unpainted specimens. Rr_s of unpainted specimens of the 90° and 45° (in-plane shear) directions show lower values than those of the 0° direction, while Rr_s of painted specimens

do not. It is thought that the surface coating prevented the painted specimens from deteriorating by comparing these results to the results of the retention ratios of the unpainted specimens. The surface coating seemed to reduce the effect of moisture because it is one of the key factors of deterioration for pultruded GFRP, such as the reduction of bending strength [13] and mass loss [14].

Table 7. Tensile and in-plane shear strengths of painted specimens with retention ratios.

Testing Direction	Code	Tensile Strength (MPa); Coefficient of Variation, CV			Retention Ratio, Rr_s	
		0 Years	1 Year	10 Years	1 Year	10 Years
0°	R43	409.6; CV _{ts} : 21.0%	496.7; CV _{ts} : 3.3%	488.0; CV _{ts} : 2.6%	1.21	1.19
	R26	369.0; CV _{ts} : 3.6%	372.4; CV _{ts} : 3.1%	316.4; CV _{ts} : 4.9%	1.01	0.86
	R12	319.2; CV _{ts} : 4.6%	330.5; CV _{ts} : 10.7%	323.8; CV _{ts} : 6.7%	1.04	1.01
90°	R43	135.8; CV _{ts} : 2.6%	140.9; CV _{ts} : 6.3%	140.9; CV _{ts} : 3.3%	1.04	1.04
	R26	165.8; CV _{ts} : 4.3%	152.1; CV _{ts} : 2.9%	162.1; CV _{ts} : 2.1%	0.92	0.98
	R12	156.2; CV _{ts} : 3.4%	158.5; CV _{ts} : 3.0%	150.8; CV _{ts} : 2.4%	1.01	0.97
45° (In-plane shear)	R43	52.6; CV _{ss} : 3.4%	50.1; CV _{ss} : 2.0%	49.0; CV _{ss} : 0.5%	0.95	0.93
	R26	56.9; CV _{ss} : 0.8%	64.6; CV _{ss} : 3.0%	70.8; CV _{ss} : 2.5%	1.13	1.24
	R12	58.0; CV _{ss} : 4.5%	57.6; CV _{ss} : 2.6%	58.9; CV _{ss} : 1.2%	0.99	1.02

Note that five coupons were used for each test.

Table 8 shows the elastic modulus of painted specimens with the retentions ratios. In the case of one year, Rr_m shows a range from 0.89 to 1.20, and CV_{tm} and CV_{sm} range from 1.8% to 7.9%. In the case of 10 years, the retention ratios show a range from 0.96 to 1.21, and CV_{tm} and CV_{sm} range from 1.7% to 5.0%. Overall, Rr_m of painted specimens is higher than those of the tensile and in-plane shear strengths, which is the same tendency as in the case of unpainted specimens.

Table 8. Elastic modulus of painted specimens with retention ratios.

Testing Direction	Code	Elastic Modulus (GPa); Coefficient of Variation, CV			Retention Ratio, Rr_m	
		0 Years	1 Year	10 Years	1 Year	10 Years
0°	R43	20.9; CV _{tm} : 12.3%	25.0; CV _{tm} : 3.8%	25.2; CV _{tm} : 3.4%	1.20	1.21
	R26	19.2; CV _{tm} : 4.3%	20.7; CV _{tm} : 2.0%	18.5; CV _{tm} : 4.3%	1.08	0.96
	R12	17.9; CV _{tm} : 2.5%	19.5; CV _{tm} : 7.9%	19.0; CV _{tm} : 4.4%	1.09	1.06
90°	R43	12.5; CV _{tm} : 2.5%	13.1; CV _{tm} : 2.5%	13.8; CV _{tm} : 1.8%	1.05	1.10
	R26	12.9; CV _{tm} : 4.0%	11.5; CV _{tm} : 4.3%	14.0; CV _{tm} : 3.1%	0.89	1.08
	R12	12.8; CV _{tm} : 2.3%	13.8; CV _{tm} : 2.6%	13.7; CV _{tm} : 1.7%	1.08	1.07
45° (In-plane shear)	R43	3.40; CV _{sm} : 3.4%	4.03; CV _{sm} : 3.7%	3.99; CV _{sm} : 2.6%	1.19	1.17
	R26	3.76; CV _{sm} : 1.7%	4.49; CV _{sm} : 7.7%	4.44; CV _{sm} : 5.0%	1.19	1.18
	R12	3.49; CV _{sm} : 2.9%	4.11; CV _{sm} : 1.8%	4.12; CV _{sm} : 3.3%	1.18	1.18

Note that five coupons were used for each test.

Figure 6 summarizes the results of the painted specimens. In contrast to the case of the unpainted specimens, the strength of the painted specimens after 10 years of outdoor exposure indicates a close value to the one before outdoor exposure, as shown in Table 7. It is thought that a surface coating can prevent the plain-woven cloth layers from deteriorating due to outdoor exposure. The elastic modulus of the painted specimens shows a slight increase as shown in Table 8, which is also observed in the case of the unpainted specimens.

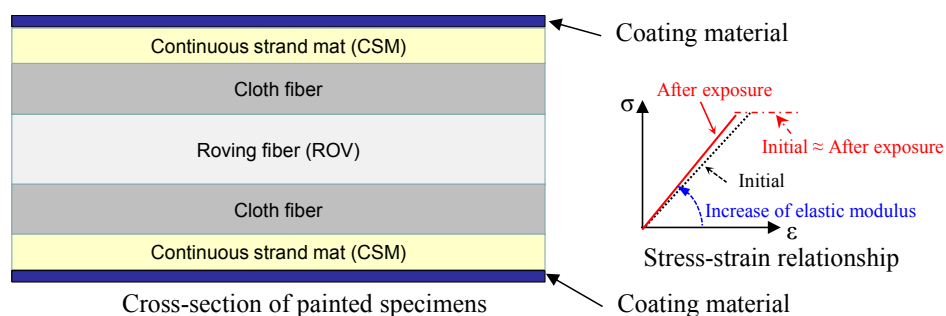


Figure 6. Summary of results of painted specimens.

4. Conclusions

The main conclusions from the present study can be summarized as follows:

In the case of the unpainted specimens, the tensile and in-plane shear strengths after 10 years of outdoor exposure were lower than those of the ones before the exposure test. By calculating the contribution ratios of each layer, plain-woven cloth, which had a relatively higher contribution ratio than the other layers, seemed to deteriorate during the 10-year exposure. For the elastic modulus of the unpainted specimens, a slight increase was observed, probably due to the effect of post-curing of the resin.

In the case of the painted specimens, the tensile and in-plane shear strengths after 10 years of outdoor exposure were close to the ones before the exposure test, which were caused by the effect of the surface paint. However, further studies are needed to understand how the surface paint protects the painted specimens. For the elastic modulus of the painted specimens, as they have the same tendency as the unpainted specimens, a slight increase was observed.

Acknowledgments: The authors gratefully acknowledge the assistance by Asahi Glass Matex Co., Ltd. for providing the specimens.

Author Contributions: The authors dedicated themselves to conduct this experimental work. Itaru Nishizaki planned and supervised the entire experimental work, and Tomonori Tomiyama prepared the specimens and placed at the exposure sites. Hiroki Sakuraba conducted the material tests and analyzed experimental results. All the authors edited the manuscript especially on their tasks.

Conflicts of Interest: The authors declare no conflict of interest.

References

1. Bulmanis, V.N.; Urzhumtsev, V.S. Effect of Cold Climate Factors on Strength and Durability of Structural Fiberglass Composites. In *ICCM & ECCM: Sixth International Conference on Composite Materials and Second European Conference on Composite Materials*; Elsevier Applied Science: London, United Kingdom, 1987; Volume 4, pp. 4.457–4.466.
2. Chin, J.W.; Nguyen, T.; Aouadi, K. Effects of environmental exposure on fiber-reinforced plastics (FRP) materials used in construction. *J. Compos. Technol. Res.* **1997**, *19*, 205–213.
3. Gentry, T.R.; Bank, L.C.; Barkatt, A.; Prian, L. Accelerated test methods to determine the long-term behavior of composite highway structures subject to environmental loading. *J. Compos. Technol. Res.* **1998**, *20*, 38–50.

4. Sridharan, S.; Zureick, A.-H.; Muzzy, J.D. Effect of hot-wet environments on e-glass/vinylester composites. In Proceedings of the 56th Society of Plastics Engineers, Annual Technical Conference, Atlanta, GA, USA, 26 April–1 May 1998; Volume 56, pp. 2255–2259.
5. Verghese, K.N.E.; Hayes, M.D.; Garcia, K.; Carrier, C.; Wood, J.; Riffle, J.R.; Lesko, J.J. Influence of matrix chemistry on the short term hydrothermal aging of vinyl ester matrix and composites under both isothermal and thermal spiking conditions. *J. Compos. Mater.* **1999**, *33*, 1918–1938. [[CrossRef](#)]
6. Kim, Y.H.; Trejo, D.; Gardoni, P. Time-variant reliability analysis and flexural design of GFRP-reinforced bridge decks. *J. Compos. Constr.* **2012**, *16*, 359–370. [[CrossRef](#)]
7. Gardoni, P.; Trejo, D.; Kim, Y.H. Time-variant strength capacity model for GFRP bars embedded in concrete. *ASCE J. Eng. Mech.* **2013**, *139*, 1435–1445.
8. Eskim, E.A.; Kolesnik, K.I.; Petrov, A.S.; Startsev, O.V.; Meletov, V.P. Некоторые особенности изменения физико-механических свойств материала типа ССТФ при старении в условиях влажных субтропиков. (In Russian).
9. Cope, R.; Revirand, G. Short term weathering of polymeric materials. *Durab. Build. Mater.* **1983**, *1*, 225–240.
10. Martin, K.G.; Sasnaitis, I. Assessment of deterioration of translucent plastics building sheets after weathering. *Durab. Build. Mater.* **1986**, *3*, 233–253.
11. Nishizaki, I.; Kishima, T.; Sasaki, I. Deterioration of mechanical properties of pultruded FRP through exposure tests. In Proceedings of the Third International Conference on Durability and Field Applications of Fibre Reinforced Polymer (FRP) Composites for Construction (CDCC2007), Quebec City, Que., Canada, 23–25 May 2007; pp. 159–166.
12. Uemura, M.; Somiya, S.; Yamatsuta, K.; Noguchi, K.; Onitsuka, T.; Honma, S.; Miyairi, Y.; Tanaka, K.; Kubota, I.; Nishimoto, T.; *et al.* *FRP Structural Design Handbook*; The Japan Reinforced Plastics Society: Tokyo, Japan, 1994; p. 31. (In Japanese)
13. Nishizaki, I.; Meiarashi, S. Long-term deterioration of GFRP in water and moist environment. *J. Compos. Constr.* **2002**, *6*, 21–27. [[CrossRef](#)]
14. Jiang, X.; Kolstein, H.; Bijlaard, F.S.K. Moisture diffusion and hygrothermal aging in pultruded fibre reinforced polymer composites of bridge decks. *Mater. Des.* **2012**, *37*, 304–312. [[CrossRef](#)]



© 2015 by the authors; licensee MDPI, Basel, Switzerland. This article is an open access article distributed under the terms and conditions of the Creative Commons by Attribution (CC-BY) license (<http://creativecommons.org/licenses/by/4.0/>).